NeuroImage: Clinical 34 (2022) 103006

Contents lists available at ScienceDirect

NeuroImage: Clinical

journal homepage: www.elsevier.com/locate/ynicl

Multiple sclerosis lesions and atrophy in the spinal cord: Distribution across vertebral levels and correlation with disability

Matthias Bussas [a,b,1], Malek El Husseini [c,1], Laura Harabacz [a], Viktor Pineker [c], Sophia Grahl [a,b], Viola Pongratz [a,b], Achim Berthele [a], Isabelle Riederer [c], Claus Zimmer [c], Bernhard Hemmer [a,d], Jan S. Kirschke [c,1], Mark Mühlau [a,b,1,*]

[a] Dept. of Neurology, School of Medicine, Technical University of Munich, Munich, Germany
[b] TUM-Neuroimaging Center, School of Medicine, Technical University of Munich, Munich, Germany
[c] Dept. of Neuroradiology, School of Medicine, Technical University of Munich, Munich, Germany
[d] Munich Cluster for Systems Neurology (SyNergy), Munich, Germany

ARTICLE INFO

Keywords:
Spinal cord
Spinal cord lesions
Spinal cord atrophy
Multiple sclerosis

ABSTRACT

Background: The vast majority of magnetic resonance imaging (MRI) studies on multiple sclerosis (MS) covered the spinal cord (SC), if at all, incompletely.
Objective: To assess SC involvement in MS, as detectable by whole SC MRI, with regard to distribution across vertebral levels and relation to clinical phenotypes and disability.
Methods: We investigated SC MRI with sagittal and axial coverage. Analyzed were brain and SC MRI scans of 17 healthy controls (HC) and of 370 patients with either clinically isolated syndrome (CIS, 27), relapsing remitting MS (RRMS, 303) or progressive MS (PMS, 40). Across vertebral levels, cross-sectional areas were semi-automatically segmented, and lesions manually delineated.
Results: The frequency of SC lesions was highest at the level C3-4. The volume of SC lesions increased from CIS to RRMS, and from RRMS to PMS whereas lesion distribution across SC levels did not differ. SC atrophy was demonstrated in RRMS and, to a higher degree, in PMS; apart from an accentuation at the level C3-4, it was evenly distributed across SC levels. SC lesions and atrophy volume were not correlated with each other and were independently associated with disability.
Conclusion: SC lesions and atrophy already exist at the stage of RRMS in the whole SC with an accentuation in the cervical enlargement; SC lesions and atrophy are more pronounced in the stage of PMS. Both contribute to the clinical picture but are largely independent.

1. Introduction

Multiple sclerosis (MS) is an autoimmune inflammatory disease of the central nervous system affecting both the brain and spinal cord (SC). Demyelinating lesions are easy to visualize by magnetic resonance imaging (MRI) even in the individual patient at the early stage, whereas the detection of atrophy at the early stage usually requires analyses across or between groups. The majority of MRI studies on MS have focused on the brain, although the SC contributes to disability in MS (Kearney et al., 2015b). SC MRI is more challenging because of the smaller anatomical size of the SC compared to the brain and because of the greater proneness to artifacts of SC MRI compared to brain MRI. Early MRI studies on SC changes in MS have suggested selective planimetric measures from axial slices as surrogate of disease progression (Losseff et al., 1996) possibly reflecting axonal loss (Lycklama et al., 2003). Later, numerous studies were performed and even *meta*-analyzed. SC atrophy seems to be greater in progressive MS (PMS) than in relapsing-remitting MS (RRMS) and to correlate with disability (Casserly et al., 2018; Song et al., 2020). Although the contribution of SC lesions to the clinical picture is beyond doubt during demyelinating attacks (Compston and Coles, 2008), their role for long term disability is less clear. Early studies did not find such a relation (Kidd et al., 1993; Lin et al., 2003; Lycklama et al., 2003; Nijeholt et al., 1998) and a later study demonstrated a contribution of only longitudinally extensive SC lesions (Amezcua et al., 2013).

* Corresponding author at: Department of Neurology, School of Medicine, Technische Universität München, Ismaninger Str. 22, D-81675 Munich, Germany.
E-mail address: mark.muehlau@tum.de (M. Mühlau).
[1] indicate equal author contributions.

https://doi.org/10.1016/j.nicl.2022.103006
Received 18 October 2021; Received in revised form 9 April 2022; Accepted 11 April 2022
Available online 13 April 2022

However, most studies on the SC in MS covered it only in part. Of the studies with complete coverage of the SC, only few applied sagittal and axial slices, which improves detectability of SC lesions (Breckwoldt et al., 2017; Galler et al., 2016; Weier et al., 2012) and has therefore been recommended (Kearney et al., 2015b). It also enables precise determination of atrophy across the whole SC (Klein et al., 2011; Mina et al., 2021) and of SC lesion load. In this retrospective cohort study, we investigated a large cohort of patients with available SC MRI, covering the SC down to the conus medullaris with both sagittal and axial slices, to assess SC lesions and atrophy with regard to the distribution across vertebral levels, association with clinical phenotypes, and correlation with disability.

2. Methods

2.1. Participants

This retrospective analysis was part of the single center cohort study on MS at the Technical University of Munich (TUM-MS), which was approved by the internal review board and performed in accordance with the Declaration of Helsinki. Patients had given written informed consent for the use of their clinical and paraclinical data for research purposes. Inclusion criteria were a diagnosis of clinically isolated syndrome (CIS) or MS, an age between 18 and 60 years, and a disease duration of <20 years. To achieve a uniform classification of patients, all patients were reclassified according to the 2017 diagnostic criteria (Thompson et al., 2018) in the context of this study. CIS patients were defined by a first clinical event suggestive of RRMS and fulfilling the criteria for dissemination in space but not fulfilling the criteria for dissemination in time. MS patients comprised those with a relapsing-remitting (RRMS) or a progressive course (PMS). Further inclusion criteria were availability of a score on the Expanded Disability Status Scale (EDSS), of a standardized quality-checked and processed brain MRI (based on a protocol exclusively used between 2009 and 2017), and of a SC MRI with coverage from the lower edge of the second vertebra to the conus medullaris in both the sagittal and axial plane. The maximum interval between either pair of the three measures (EDSS, SC MRI, brain MRI) was set to 400 days. We also defined two subgroups by the availability of further clinical scores in the same time frame. The first subgroup comprised patients with available scores at the Nine-Hole Peg Test (Feys et al., 2017) and 25-Foot Walk Test (Motl et al., 2017). The second subgroup comprised patients with an available score at the Multiple Sclerosis Inventory of Cognition (MuSIC), which yields one score for cognition ranging from zero to 30 and one score for fatigue ranging from three to 21 (Calabrese et al., 2004; Yaldizli et al., 2014).

SC MRI data of the healthy controls (HC) were taken from our in-house database. These subjects were scanned in the context of medical examinations performed because of symptoms that retrospectively could not be related to a severe or chronic neurological disorder (e.g., transient sensory symptoms due to mechanical irritation of a peripheral nerve).

2.2. MRI acquisition and processing

SC MRI was performed on several scanners, but we finally restricted our analyses to three 3-Tesla scanners (Philips Ingenia, Philips Achieva dStream, Siemens Magnetom Verio) that contributed to > 90% of the data. A spine coil was used and optionally an anterior body coil. All scans included 2D T2-weighted (w) turbo spin echo sequences in sagittal and axial orientation. Sagittal scans had a slice thickness of 2 mm with a gap of 0.2 mm, axial scans had a slice thickness of 4 mm with a gap of 1 mm. Typical field of view (FOV) of axial scans was 115 mm with an in-plane spatial resolution of 0.4 mm (ranging from 0.3 mm to 0.5 mm); they were acquired in three consecutive stacks. Sagittal scans had a typical FOV of 250 mm with an in-plane spatial resolution of 0.9 mm (ranging from 0.8 mm to 1 mm). An overview on our in-house processing pipeline is given in Fig. 1. All scans were converted to NIFTI file format and segmented with the software BrainSeg3D, Version 2.2.1 (https://lit.fe.uni-lj.si/tools.php?lang = eng). First, we segmented the SC area in axial scans using a region-growing algorithm that had to be initialized by manual setting of a seed point within the SC in each slice.

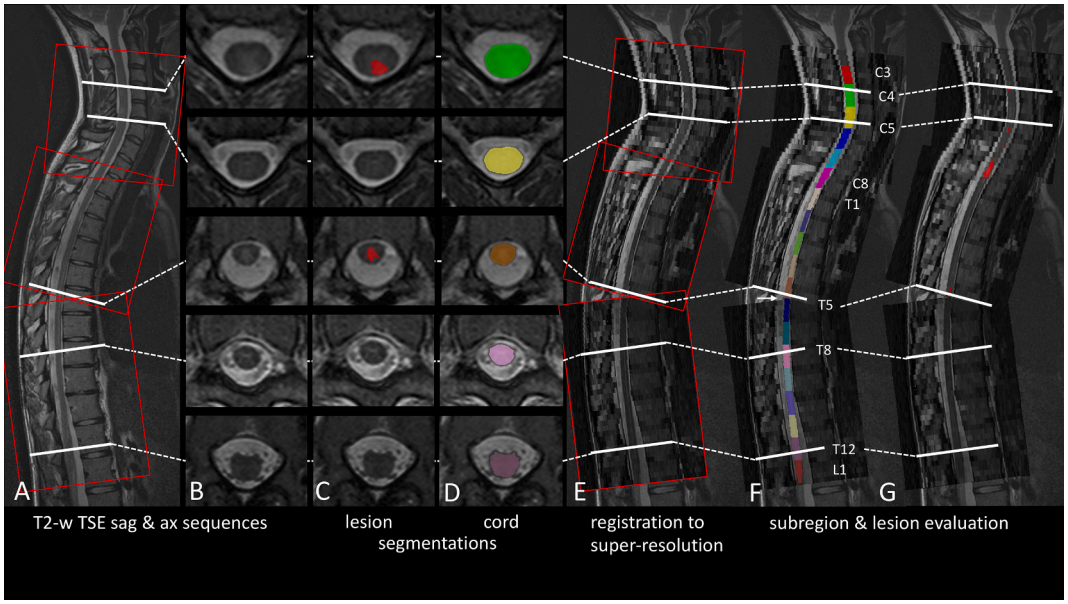

Fig. 1. Processing pipeline for spinal cord images. (A) Median sagittal (sag) slice of a native T2-weighted (TSE, turbo spin echo) sequence is shown. Red rectangles correspond to the three stacks of the axial sequence. White lines correspond to axial (ax) slices in B, C, and D. (B/C/D) Axial slices of T2-weighted (turbo spin echo) images are shown (B, native; C, after manual lesion segmentation; D, spinal cord segmentation. (E) Registration of axial and sagittal images to a common space. (F) From the caudal end of vertebra C2 to the conus, the spinal cord was divided into 19 equal segments along the spinal cord centerline. These segments correspond to the levels labeled C3-C8, T1-T12, and L1. For regions not covered by axial slices (arrow), spinal cord segmentation was interpolated. (G) Lesion segmentation after transformation into a common space. Note that segmentation was first performed based on the axial slices, but that later calculation of level-wise volumes (spinal cord and lesions) was performed in the common space for attribution of volumes to spinal cord segments. (For interpretation of the references to color in this figure legend, the reader is referred to the web version of this article.)

Manual corrections of the outline were performed when necessary. Lesions were segmented fully manually. This segmentation was performed by two medical students (LH and VP). To achieve a consensus segmentation, they consulted a senior neuroradiologist (JK) when they were uncertain or when their lesion segmentation did not match with the written neuroradiological report. After an intensive training period supervised by JK, we performed a cross-validation (LH and VP) in 25 patients, of whom 15 had SC lesions, indicating very good agreement (mean voxel-wise Dice coefficient of atrophy/lesions: 0.98/0.79). Additionally, the lower edge of the second cervical vertebra (C2) as well as the conus medullaris were separately marked in the sagittal images. These segmentations were evaluated using an in-house python-based algorithm. We registered axial and sagittal scans with the software SimpleITK v1.20 to obtain one common space per patient with an isotropic resolution of 0.5 mm. In this space, we also registered segmentations of the axial slices. The stacks of the axial slices covered the SC from the lower edge of vertebra C2 to the conus medullaris in most cases. As acquisitions were planned manually in clinical routine, few slices were missed in some cases; the regions T6 and T7 (border between middle and caudal stack), and L1 (conus medullaris) were covered by $>$ 90% and the remaining regions by $>$ 95%. To account for gaps between stacks, we linearly interpolated the curvature and thickness of the missing region. The common space of axial and sagittal slices, covering the full SC, was subdivided in 19 regions between the C2 landmark and the conus medullaris. Division into 19 equally large regions was based on the total stretched length of the skeletonized spine along the craniocaudal axis (i.e., the spinal centerline). As lower anatomical landmark, we preferred the conus medullaris over adjacent vertebrae, as the position of the conus medullaris shows a substantial variation in location between T12 and L2 even in healthy controls (Qu et al., 2017) so that the lumbar enlargement might not be co-registered precisely across subjects. In analogy to the nerve roots, these 19 regions were named C3-C8, T1-T12, and L1. Assuming equal distances between the root entry zones of the SC, which is roughly the case in the upper SC, a region labelled [C or T]x approximately covers the part of the SC between the entry zones of the roots [C or T]x and [C or T]x + 1, whereas the maximum of the lumbar enlargement corresponds to T11. These topographic relations of our 19 segments were confirmed by thorough visual inspection of our images. To account for body size (Healy et al., 2012; Oh et al., 2014), the mean cross-sectional area in mm^2 (perpendicular to the centerline) was calculated per region. The mean of these 19 values, the mean cross-sectional area, was taken as a normalized volume measure of the whole SC. Lesion volumes of all 19 regions were calculated and summed up.

Brain MRI was performed at a 3 Tesla scanner Achieva (Philips Medical Systems, Netherlands). Standardized brain MRI comprised a 3D spoiled gradient echo T1-weighted (T1w) sequence (voxel size = 1 mm isotropic, TR = 9 ms, TE = 4 ms) and a turbo-spin echo T2-weighted fluid-attenuated inversion recovery sequence (voxel size = 1.0 × 1.0 × 1.5 mm, TR = 10,000 ms, TE = 140 ms, TI = 2750 ms). Brain images were processed with the software package SPM12 and its toolboxes CAT12 (Computational Anatomy Toolbox, version 916, https://www.neuro.uni-jena.de/cat12/) and LST (lesion segmentation tool, version 2.0.15, https://www.applied-statistics.de/). White matter (WM) lesions were segmented from FLAIR and T1-weighted images by the lesion growth algorithm (Schmidt et al., 2012) as implemented in LST. After lesion filling, as implemented in LST, we applied CAT12 to generate normalized images of grey matter (GM), WM, and cerebrospinal fluid. Brain volume was calculated by the sum of brain WM and GM. Total intracranial volume was determined by a reverse brain mask approach (Keihaninejad et al., 2010).

2.3. Statistical analysis

To approach normal distribution and for visualization, the natural logarithm of brain and SC lesion volumes was calculated. To avoid negative values, 1 was added to volumes in μL beforehand. For group comparisons, we used t-tests for all pairs of groups. Global volumes are illustrated by violin plots. Plots across SC levels display mean values and their standard error. SC lesion incidence across vertebral levels (percentage of patients with lesions) is illustrated by a frequency plot. To correlate SC (and brain) parameters with clinical scores, CIS and RRMS patients were assigned to one group (for the relatively low number of CIS patients). We applied simple and partial correlation models. The latter were performed at two levels. At each level, one clinical score served as response variable and age, sex, disease duration, total intracranial volume, and scanner (three scanners modelled by one factor variable with three levels) as explanatory variables that were regarded as control variables. At the first level (partial-1), one out of four explanatory variables of interest was included, namely either SC lesion volume, or SC volume (atrophy), or brain WM lesion volume, or brain volume (atrophy); this resulted in four partial correlation models. At the second level (partial-2), all of the same four explanatory variables of interest were included as explanatory variables of interest, this resulted in one further partial correlation model. The correlation models resulted in 4 × 16 statistical tests that were, however, not independent. To address the issue of multiple statistical tests, we applied a statistical threshold of $p < 0.001$, corresponding to 50 independent tests, but also reported the uncorrected p values. Moreover, clinical scores were correlated to level-wise SC measures. As these analyses were primarily performed to localize effects identified by the correlation models, only simple correlations using Spearman's rank correlation coefficient without corrections for multiple comparisons were performed. All analyses were performed with the software R (version 3.6.3); plots were generated with its package ggplot2.

3. Results

3.1. Study participants

From our database, we identified 556 patients aged between 18 and 60 years with an established diagnosis of CIS or MS, with a disease duration of <20 years, at least one SC MRI, one well-processed and quality-checked brain MRI, and one documented EDSS score (the latter two within the predefined interval of 400 days). Since three 3 Tesla scanners contributed to $>$ 90% of all images, we restricted the dataset for analysis to these three scanners. Of the 556 preselected SCI MRI, 404 were acquired at one of the three scanners and showed sagittal and axial coverage at least from the lower edge of C2 to the conus medullaris. Because of poor image quality, 34 SC MRI were excluded during image processing resulting in 370 datasets for analysis. We also identified 20 suitable HC with available SC MRI (including the required coverage); of these, three were excluded during image processing because of poor image quality. Key characteristics of the final cohort are summarized in Table 1.

3.2. Spinal cord lesion volumes and atrophy across vertebral levels

Whole SC lesion volumes (Fig. 2A) differed between groups increasing from HC (none) to CIS ($p < 0.05$), from CIS to RRMS ($p < 0.001$), and from RRMS to PMS ($p < 0.001$). These differences were observed across almost all vertebral levels; among the groups of CIS, RRMS, and PMS, we observed a similar spatial distribution of lesions with the highest frequency at the level C4 (Fig. 2B). Frequency plots across vertebral levels showed a comparable behavior (Fig. 2C). Whole SC atrophy was observed in PMS (Fig. 3A) compared to all other groups ($p < 0.001$). The remaining pair-wise comparisons yielded one further significant result, namely smaller mean SC areas in RRMS compared to HC ($p = 0.01$). Across vertebral levels, both absolute (Fig. 3B) and relative (Fig. 3C) differences were most pronounced at the cervical enlargement.

Table 1
Key characteristics of participants.

	Control subjects	CIS	RRMS	PMS	CIS, RRMS, and PMS
N	17	27	303	40	370
EDSS		27	303	40	370
9HPeg and 25FWalk		14	214	17	245
MuSIC		13	195	8	216
Females	11	14	209	22	245
(%)	(65%)	(52%)	(69%)	(55%)	(66%)
Age	28.6 ± 6.1	35.4 ± 9.9	35.0 ± 9.1	47.7 ± 6.9	36.4 ± 9.8
in years	28.5	35.4	34.8	47.9	35.9
	[20.8–43.3]	[20.1–55.4]	[18.0–59.5]	[31.5–59.6]	[18.0–59.6]
Disease duration		0.4 ± 0.8	2.8 ± 4.5	8.3 ± 5.8	3.2 ± 4.9
in years		0.08	0.5	6.4	0.6
		[0.02–3.3]	[0.0–19.6]	[1.0–19.9]	[0.0–19.9]
Patients with at least one SC lesion N (%)	0	6	230	36	272
	(0%)	(22%)	(76%)	(90%)	(74%)
EDSS	n.d.	1.2 ± 1.0	1.6 ± 1.4	5.1 ± 1.8	1.9 ± 1.8
		1.0 [0.0–3.5]	1.5 [0.0–8.5]	5.2 [1.5–9.0]	1.5 [0.0–9.0]
9HPeg	n.d.	17.8 ± 2.6	19.0 ± 4.4	24.2 ± 7.5	19.3 ± 4.8
		16.9	18.2	22.8	18.2
		[14.2–23.6]	[13.5–54.5]	[17.0–49.8]	[13.5–54.5]
25FWalk	n.d.	3.9 ± 0.7	4.4 ± 1.1	9.3 ± 7.1	4.7 ± 2.5
		4.1	4.2	6.9	4.2
		[2.7–5.1]	[2.5–14.0]	[3.6–29.8]	[2.5–29.8]
Cognition	n.d.	25.8 ± 4.1	25.7 ± 4.0	19.8 ± 3.7	25.5 ± 4.1
(MuSIC)		26.0 [14–30]	26.0 [10–30]	20.0 [15–26]	26.0 [10–30]
Fatigue	n.d.	6.0 ± 3.5	7.9 ± 4.5	11.9 ± 4.6	7.9 ± 4.5
(MuSIC)		4.0 [3–13]	7.0 [3–21]	12.5 [3–17]	7.0 [3–21]
Disease modifying drugs	/				
None/DMF/FTY/		26/0/0	244/4/6	31/1/0	301/5/6
Glat/INF/Mitox/		0/1/0	16/27/0	1/3/1	17/31/1
NTZ/RTX/Sin		0/0/0	6/0/0	1/1/1	7/1/1
Scanner					
Achieva/Ingenia/ Verio	13/2	14/2	191/16	29/2	234/20
	2	11	96	9	116

Values are given in mean ± standard deviation and in median [range].
9HPeg, Nine-Hole Peg Test; 25FWalk, 25-Foot Walk Test; CIS, clinically isolated syndrome; DMF, Dimethyl fumarate; EDSS, Expanded Disability Status Scale; FTY, Fingolimod; Glat, Glatiramer acetate; INF, Interferon ß; Mitox, Mitoxantrone; MuSIC, Multiple Sclerosis Inventory Cognition; n.d., not determined; NTZ, Natalizumab; PMS, progressive multiple sclerosis; RRMS, relapsing-remitting multiple sclerosis; RTX, Rituximab; SC, spinal cord; Sin, steroids in intervals, i.e. pulsed methylprednisolone therapy.

3.3. Relation of spinal cord lesions and atrophy

Global values of SC lesions and atrophy did not correlate with each other in the whole cohort (Pearson's $r = -0.005, p = 0.9$). Unexpectedly, such a relation was not even observed when comparing the 99 patients without any SC lesion (i.e., a SC lesion volume of zero) to those 99 patients with the largest SC lesion volume (t-test, $p = 0.7$). Plots of SC mean cross-sectional areas across vertebral levels, separately for both groups, neither suggested such a relation at any SC level (Fig. 4).

3.4. Associations of disability and MRI measures across phenotypes of MS

Simple and partial correlation models of all four global MRI parameters of interest (SC lesions, SC atrophy/volume, brain WM lesions, brain atrophy/volume) with EDSS and demographic parameters are shown in Table 2. Simple correlations with EDSS yielded significant associations of all four MRI parameters of interest across the whole group of patients and of SC lesion volume within the CIS/RRMS group. The association of level-wise SC lesion volumes with EDSS was significant with similar effect sizes (standardized correlation coefficient ß) across vertebral levels and groups (Fig. 5A); the smaller group of patients with PMS showed large confidence intervals. SC atrophy was significantly associated with EDSS only across the whole group of patients. Caudally, the strength of this association decreased (Fig. 5B). Partial correlation analyses of whole brain and whole SC MRI parameters of interest gave a similar picture (Table 2). Again, the association of SC lesions with EDSS was robust in the CIS/RRMS group and across the whole group; however, the association of SC atrophy with EDSS lost significance even in the whole group. Common models, including all four MRI parameters of interest, yielded significant independent contributions of only SC lesions, and brain WM lesions.

3.5. Associations of clinical scores and MRI measures

Simple correlation models of all four global MRI parameters of interest with further clinical scores across the whole patient group are shown in Table 2. The 25-Foot Walk test was associated with all four MRI parameters of interest. In contrast to EDSS, the 25-Foot Walk test showed a stronger association with SC atrophy than with SC lesion volume; further, SC atrophy was the only parameter that showed an independent contribution in the partial correlation model with all four global MRI parameters of interest (partial-2). Plots across the SC levels show a similar picture (Fig. 6). Although EDSS and 25-Foot Walk test behave similarly, the curve of the EDSS indicates stronger associations with SC lesions than the curve of the 25-Foot Walk test (Fig. 6A); yet regarding SC atrophy, the curves of EDSS and 25-Foot Walk test show the opposite behavior (Fig. 6B). Motor hand arm function, as measured by the 9-Hole Peg test, was associated with SC lesions in an anatomically plausible way, namely stronger in the upper SC, whereas no association with SC atrophy was observed. We did not observe an association of fatigue with any MRI parameter of interest.

4. Discussion

This study investigated a large cohort of patients with CIS or MS through SC MRI with sagittal and axial coverage down to the conus medullaris. SC lesions and atrophy independently occurred at all SC levels but were accentuated at the cervical enlargement. SC lesions

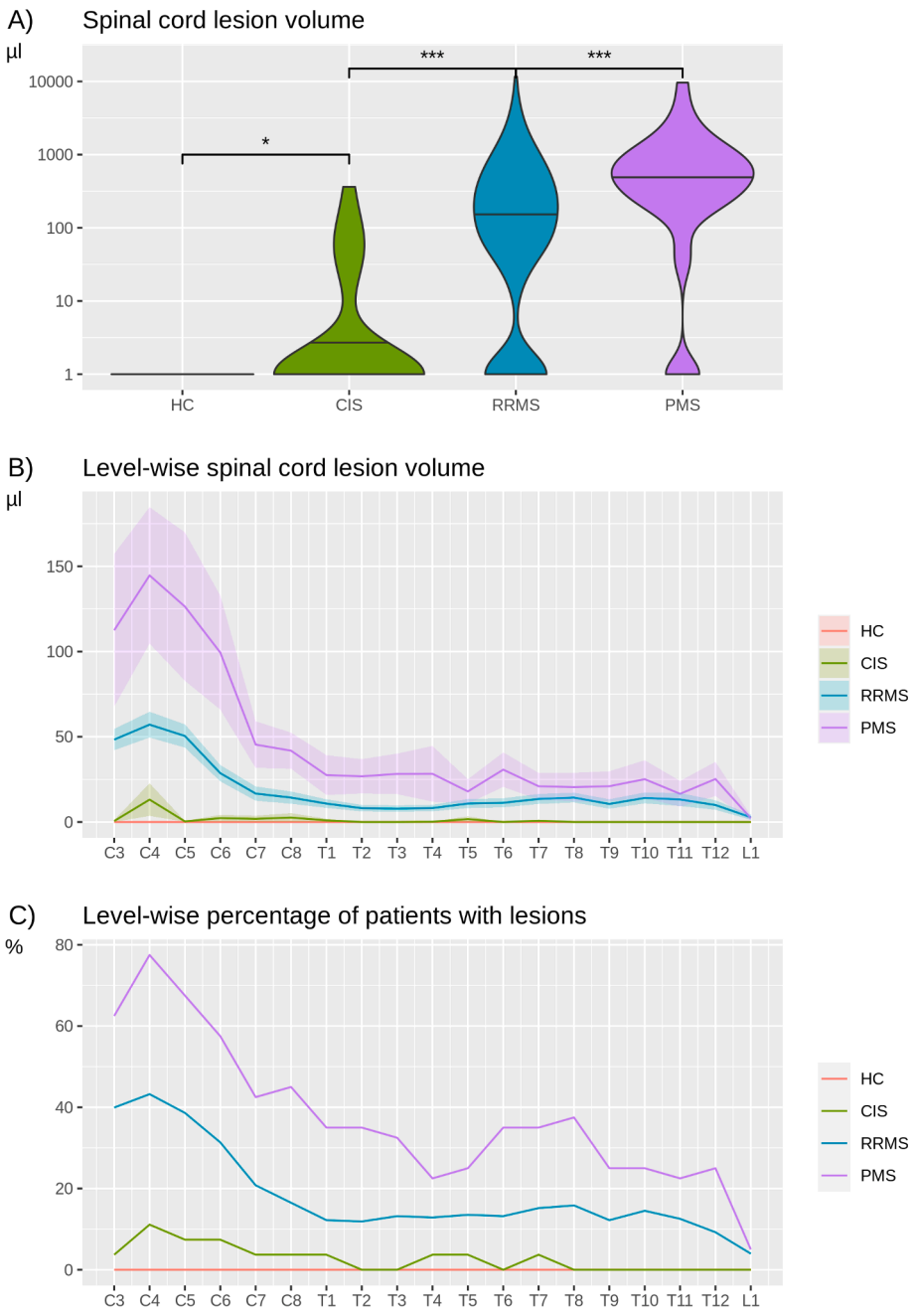

Fig. 2. Spinal cord lesions across vertebral levels. (A) Violin plots show spinal cord (SC) lesion volumes across groups (HC, healthy controls; CIS, clinically isolated syndrome; RRMS, relapsing-remitting multiple sclerosis; PMS, progressive multiple sclerosis). Note the logarithmic scale of the y axis. Statistical significance is marked by asterisks ($p < 0.05$, *; $p < 0.01$, **; $p < 0.001$, ***). (B) Mean volumes and standard error of SC lesions on the y axis are plotted across vertebral levels on the x axis (C, cervical; T, thoracic; L, lumbar) separately for HC (no lesions), CIS, RRMS, and PMS. Level-wise statistical significance is indicated by non-overlapping confidence intervals. (C) Frequency plots show the percentage of patients with at least one lesion across SC levels, separately for HC, CIS, RRMS, and PMS.

contribute to the clinical picture in RRMS and PMS, whereas SC atrophy becomes detectable in RRMS but seems to contribute to the clinical picture later. We will discuss the characteristics of our cohort, the spatial distribution of SC lesions and atrophy and their interplay, as well as the contribution of SC lesions and atrophy to the clinical picture; finally, we will acknowledge limitations of our study and give an outlook.

Our cohort comprised a relatively high number of patients scanned in the clinical context of a tertiary center mostly to confirm the diagnosis of MS. Our SC MRI protocol lasts longer than 30 min. According to our experience, we operate at the edge of feasibility in clinical routine with regard to the requirements for patients' compliance and MRI capacity. This is also illustrated by the fact that almost 20 percent of patients assigned for SC MRI were actually not scanned across the whole SC. Despite our protocol comprising sagittal and axial coverage, the proportion of patients with at least one SC lesion was not considerably higher than in early studies (Lycklama et al., 2003). This proportion was only 25% in the patients with CIS. Of note, after reclassifying our patients according to the latest revision of the diagnostic criteria (Thompson et al., 2018), the diagnosis of CIS has become rare. Many MRI scans showed contrast-enhancing and none-enhancing lesions at a time or routinely performed lumbar puncture revealed cerebrospinal fluid specific oligoclonal bands. In consequence, many patients that had been diagnosed with CIS formerly were reclassified to RRMS in the context of this study. Therefore, we believe that our CIS group is difficult to compare to other CIS cohorts. This reclassification also changed our RRMS group, which was dominated by early stages as indicated by a median disease duration of less than a year. Still, the percentage of 74% of patients with at least one SC lesion was in the range of earlier studies reporting about 80% (Lycklama et al., 2003). Because of the low number of patients with primary and secondary PMS, we gathered these patients to one group as done by others (Bonacchi et al., 2020). This decision can be justified because of the absence of qualitative clinical (apart from the

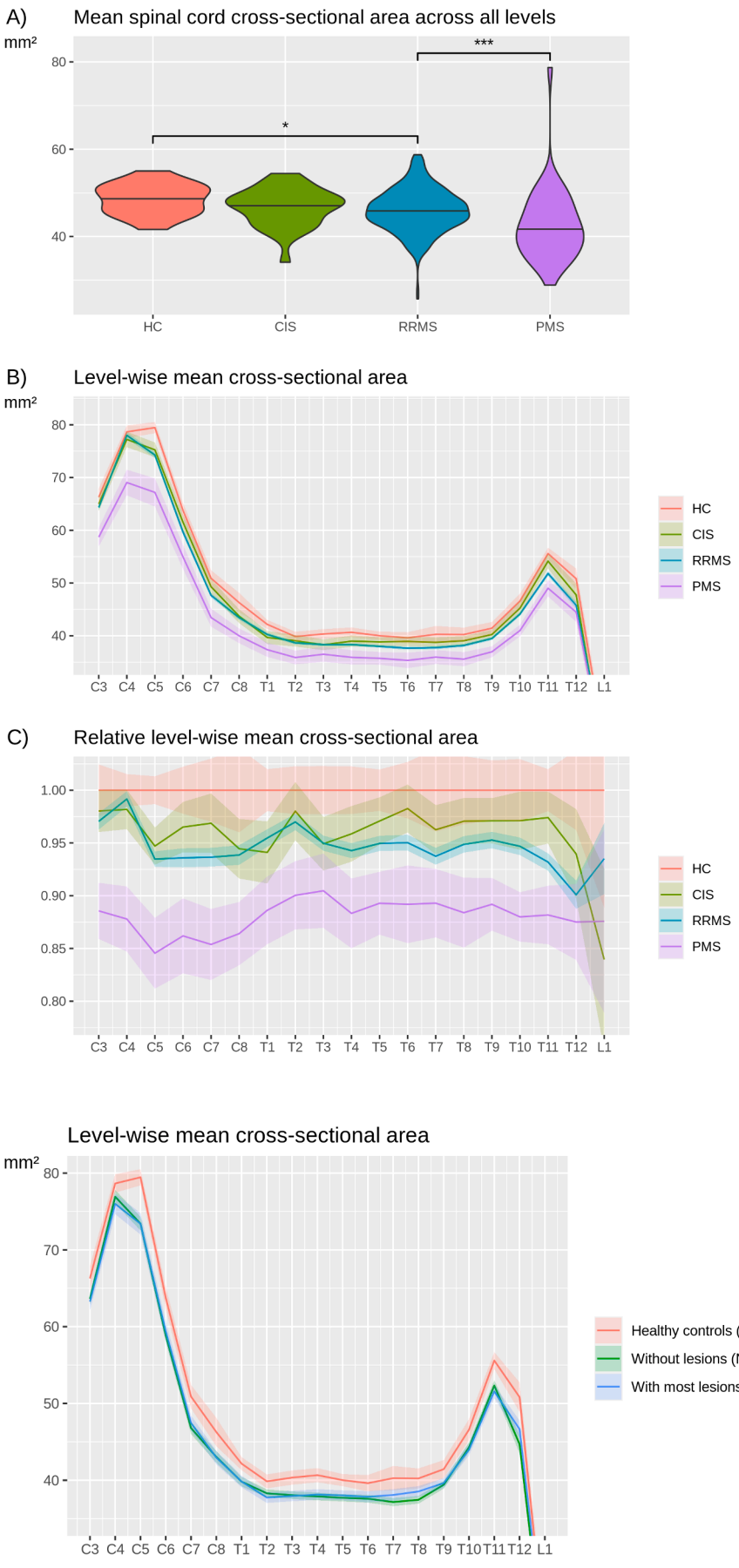

Fig. 3. Mean spinal cord cross-sectional area across vertebral levels. (A) Violin plots show spinal cord (SC) mean cross-sectional areas across groups (HC, healthy controls; CIS, clinically isolated syndrome; RRMS, relapsing-remitting multiple sclerosis; PMS, progressive multiple sclerosis). Statistical significance is marked by asterisks ($p < 0.05$, *; $p < 0.01$, **; $p < 0.001$, ***). (B) Mean SC cross-sectional areas and standard error on the y axis are plotted across SC levels on the x axis (C, cervical; T, thoracic; L, lumbar), separately for HC, CIS, RRMS, and PMS. (C) For each level, mean SC cross-sectional areas were scaled by respective means of the HC group at this level (resulting in a mean value of 1.0 for all levels in the HC group). (B/C) Level-wise statistical significance is indicated by non-overlapping confidence intervals.

Fig. 4. Comparison of spinal cord volumes between patients without any spinal cord lesion, patients with most spinal cord lesion volumes, and healthy controls. Mean spinal cord cross-sectional areas and standard error on the y axis are plotted across vertebral levels on the x axis (C, cervical; T, thoracic; L, lumbar), separately for the 99 patients without a single spinal cord lesion, the 99 patients with the highest spinal cord lesion volumes, and the 17 healthy controls. Statistical significance is indicated by non-overlapping confidence intervals.

Table 2
Simple and partial correlation analyses of clinical scores and magnetic resonance imaging measures.

	Brain Volume	Brain Lesion Volume	Spinal Cord Volume	Spinal Cord Lesion Volume
Age, all, simple	−0.1 (0.005*)	0.4 (3e-12**)	−0.01 (0.8)	0.09 (0.08)
Sex (f > m: <0), all, simple	0.5 (1e-25**)	0.1 (0.05)	0.1 (0.06)	0.1 (0.03*)
Disease Duration, all, simple	−0.2 (4e-04**)	0.4 (2e-18**)	−0.2 (7e-04**)	0.3 (1e-06**)
Intracranial V, all, simple	0.9 (6e-185**)	0.02 (0.7)	0.4 (2e-13**)	−0.02 (0.7)
Scanner	n/a	n/a	(>0.3)	(>0.9)
Brain Volume, all, partial-1	/	−0.5 (6e-26**)	0.2 (0.002*)	−0.1 (0.007*)
Brain Lesion V, all, partial-1	−0.5 (6e-26**)	/	0.04 (0.5)	0.2 (2e-06**)
SC Volume, all, partial-1	0.2 (0.002*)	0.04 (0.5)	/	0.08 (0.1)
SC Lesion V, all, partial-1	−0.1 (0.007*)	0.2 (2e-06**)	0.08 (0.1)	/
EDSS				
CIS/RRMS, simple	−0.2 (0.003*)	0.3 (1e-09**)	−0.07 (0.2)	0.3 (1e-08**)
partial-1	−0.2 (0.001*)	0.2 (4e-05**)	−0.06 (0.3)	0.3 (4e-07**)
partial-2	−0.3 (0.2)	0.1 (0.03*)	−0.07 (0.2)	0.2 (2e-05**)
PMS, simple	−0.3 (0.1)	0.4 (0.02*)	−0.07 (0.7)	0.1 (0.4)
partial-1	−0.02 (0.9)	0.2 (0.3)	0.2 (0.2)	0.1 (0.4)
partial-2	0.11 (0.9)	0.16 (0.5)	0.17 (0.5)	0.02 (0.9)
All, simple	−0.2 (2e-06**)	0.5 (5e-20**)	−0.2 (7e-04**)	0.3 (5e-12**)
partial-1	−0.2 (4e-05**)	0.3 (3e-07**)	−0.08 (0.1)	0.3 (1e-07**)
partial-2	−0.3 (0.2)	0.2 (0.004*)	−0.09 (0.06)	0.2 (9e-06**)
Further Clinical Scores (All patients)				
25FWalk, simple	−0.2 (0.002*)	0.2 (0.001*)	−0.3 (3e-05**)	0.2 (0.001*)
partial-1	−0.2 (0.01*)	0.1 (0.09)	−0.2 (0.001*)	0.1 (0.06)
partial-2	−0.4 (0.1)	0.06 (0.4)	−0.2 (9e-04**)	0.1 (0.08)
9HPeg, simple	−0.05 (0.4)	0.2 (2e-04**)	−0.01 (0.8)	0.3 (8e-06**)
partial-1	−0.1 (0.07)	0.2 (0.005*)	0.004 (1.0)	0.2 (3e-04**)
partial-2	−0.2 (0.5)	0.1 (0.07)	−0.01 (0.8)	0.2 (0.001*)
Fatigue, simple	−0.1 (0.1)	0.05 (0.4)	0.03 (0.6)	0.1 (0.2)

Effect sizes (standardized ß) and, in parentheses, p values of simple correlations ('simple') with the four volumes in interest, namely brain white matter lesion volume, brain volume, spinal cord lesion volume, and spinal cord volume are given. Effect sizes (standardized ß) and p values of partial correlations ('partial') are also given for the four volumes and for clinical scores. Partial-1 correlations include one variable of interest, namely one volume or one clinical score, and the control variables of age, sex, disease duration, (total) intracranial volume, and scanner. Partial-2 correlations additionally include the three remaining volumes. Significance is indicated by one/two asterisks ($p < 0.05/0.001$).
9HPeg, Nine-Hole Peg Test; 25FWalk, 25-Foot Walk Test; All, all patients (CIS/RRMS and PMS); ß, standardized beta; CIS/RRMS, group of patients with clinically isolated syndrome or relapsing-remitting multiple sclerosis; EDSS, Expanded Disability Status Scale; f > m: <0, higher values in women translate into negative ß values; Fatigue, score of Multiple Sclerosis Inventory Cognition; n/a, not applicable; PMS, progressive MS; SC, spinal cord; Scanner, factor variable with 3 levels, number relates to smallest p value; V, volume.

course), immunological, histopathological, or neuroimaging features differentiating both types (Filippi et al., 2020) and very similar demographic features across huge cohorts (Confavreux and Vukusic, 2006). In our PMS group, the percentage of patients with at least one SC lesion was higher, namely 90%, yet far from 100%, indicating that even when studied by full axial and sagittal coverage, some patients with PMS remain free from SC lesions. Further, our patients with PMS had a longer disease duration and were older than our patients with CIS or RRMS as in other large cohorts (Confavreux and Vukusic, 2006). This made statistical models challenging. On the one hand, these differences between groups are inherent to the different phenotypes and stages of the disease; on the other hand, findings not distinguishable from mere age effects are difficult to interpret. In addition, critical for statistical models comprising SC and brain measures is the fact that the latter correlates with age more strongly than the former. Regarding brain measures, excluding age increases the risk of false positive findings whereas including age increases the risk of false negative findings, since collinearity of variables enlarges confidence intervals and, thus, lowers statistical power. Against this backdrop, we decided to perform uncorrected tests for comparisons of phenotypes but to correct for age, sex, and disease duration in statistical models on clinical scores.

The distribution of SC lesions and atrophy across SC levels was a main objective of our study. In line with our results, further studies reported the highest frequency of lesions at the cervical enlargement (Amezcua et al., 2013; Bot et al., 2004; Breckwoldt et al., 2017; Galler et al., 2016; Kidd et al., 1993; Poulsen et al., 2021; Weier et al., 2012). Of note, a recent study focusing on lesions in the corticospinal tract, covering the brain and upper cervical SC, also reported the highest frequency at C3/4 (Kerbrat et al., 2020). We are aware of few studies reporting SC atrophy across SC levels. An early study focused on the levels around C5, T2, T7, and T11 and found most atrophy at C5 and T7 similar to our results (Kidd et al., 1993). A very recent study (Mina et al., 2021) also investigated atrophy across the whole SC. Virtually mirroring our results, both groups of patients with PMS (59 patients with primary and 49 with secondary MS) showed significant atrophy compared to controls, which was most pronounced in the cervical SC but evenly distributed in the thoracic SC. The strongest difference to our results was that RRMS patients only showed significant atrophy in the cervical SC, which may result from the lower number of RRMS patients. Given the homogeneity of atrophy, the selection of few SC levels for volumetry, as done in numerous studies (Casserly et al., 2018; Song et al., 2020), seems to be a powerful approach to investigate SC atrophy. The accentuation in the cervical enlargement, found for both measures, may be related to the high content of GM. SC GM lesions exist, and, in contrast to the brain, WM lesions frequently extend into GM disregarding the GM/WM boundary (Gilmore et al., 2006; Petrova et al., 2018). Moreover, studies using high resolution SC MRI found SC atrophy pronounced in GM (Kearney et al., 2016; Schlaeger et al., 2014; Schlaeger et al., 2015).

An interplay of SC atrophy and SC lesions was not evident in our study. Both measures appeared to be largely independent. This is compatible with an MRI study investigating the cervical cord (Kearney et al., 2015a) and histological studies as SC lesions primarily reflect demyelination (Nijeholt et al., 2001), whereas the underlying cause of SC atrophy is less clear (Evangelou et al., 2005; Petrova et al., 2018). On the other hand, studies exist that reported a more direct relation between SC lesions and atrophy (Pravatà et al., 2019; Sechi et al., 2021). Further, simply because both measures develop over time, as underlined by the high correlation with disease duration, we expected at least some degree of correlation. Nevertheless, even when we compared those 99 patients without any SC lesion to the same number of patients with the largest SC lesion volumes, we did not find a difference of SC volume, neither of the global values nor across SC levels. It seems that other factors, possibly such as the coexistence of swelling from inflammatory edema and atrophy, exert strong and differential influences and, thereby, cover the time-dependent component of both measures.

For the analyses of the relation of SC measures with clinical

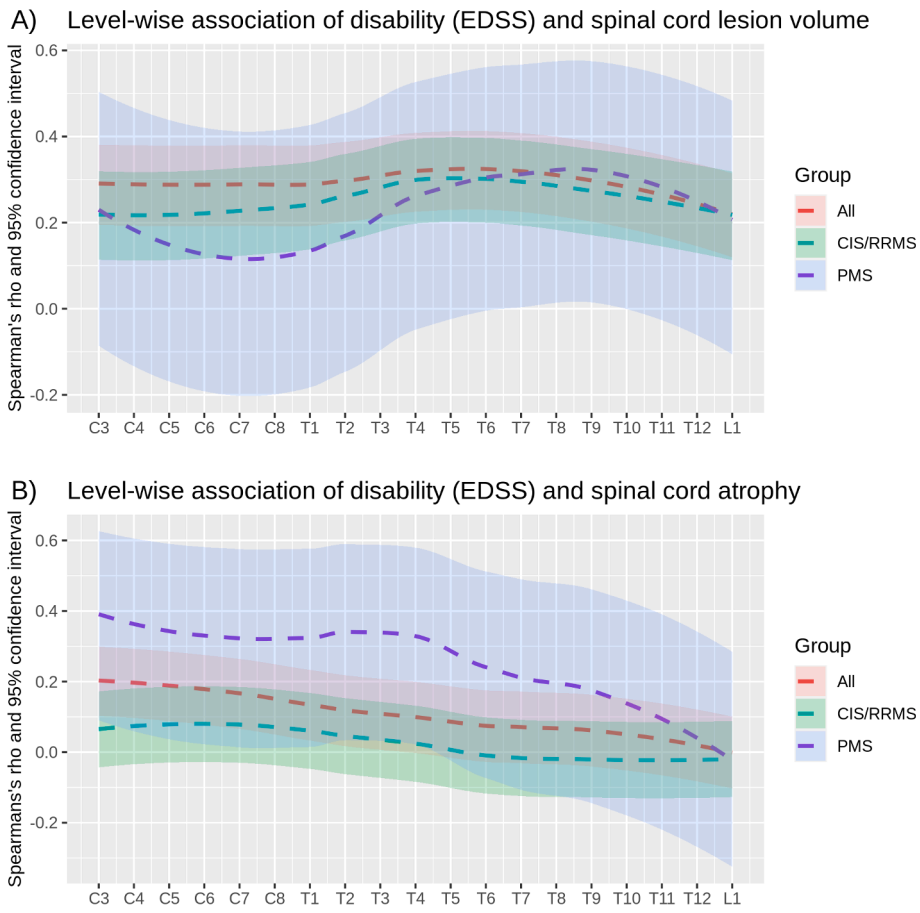

Fig. 5. Association of spinal cord lesions and atrophy with disability (EDSS) across vertebral levels. (A) Level-wise simple non-parametric correlations of scores at the Expanded Disability Status Scale (EDSS) and spinal cord lesion volumes are plotted across vertebral levels (C, cervical; T, thoracic; L, lumbar), separately for patients with clinically isolated syndrome or relapsing-remitting multiple sclerosis (CIS / RRMS), progressive MS (PMS), and all patients together. Of each group, color-coded correlation measures with their 95% confidence intervals (colored areas) are displayed. For visibility, these values were smoothed (default function of ggplot2). Level-wise statistical significance is indicated by non-overlapping of confidence intervals with zero. (B) Analogous plots derived from level-wise simple correlations of EDSS and spinal cord volumes are displayed.

phenotypes and disability, we chose a granular statistical design not to miss differences among groups and to ensure that significant associations cannot merely be attributed to collinearity among the MRI measures of interest (atrophy/volume and lesions of SC and brain). Simple correlations with both SC measures showed the strongest associations with EDSS across the whole patient group suggesting that these association play an important role throughout the course of MS (rather than at a certain stage). After correcting for other measures including MRI parameters, SC lesion volume showed an independent association with EDSS and SC atrophy with the 25-Foot Walk Test. Our results on the relation of SC measures with groups (clinical phenotypes) point toward an important role throughout the course of MS indicating SC atrophy already in RRMS and more so in PMS; differences were most pronounced at the cervical enlargement, making it an attractive region-of-interest to gain an estimate of SC atrophy. Our finding of an independent contribution of SC atrophy to a clinical score across our whole cohort is in line with other studies (Andelova et al., 2019; Mina et al., 2021; Tsagkas et al., 2018) including two *meta*-analyses (Casserly et al., 2018; Song et al., 2020). Of note, a recent longitudinal study demonstrated similar atrophy rates of the SC in RRMS and secondary PMS (Tsagkas et al., 2018). Taken together, SC atrophy appears to be a continuous process affecting the whole SC from the beginning of the disease, becoming early detectable at the group level, and contributing to the clinical picture in the later course. These relations are less clear for SC lesions. Their contribution to the clinical picture is beyond doubt during demyelinating attacks (Compston and Coles, 2008), whereas evidence on the contribution of SC lesions to sustained disability at the cohort level and, hence, to long-term disability is sparse. Early studies did not find such a relation (Kidd et al., 1993; Lin et al., 2003; Lycklama et al., 2003; Nijeholt et al., 1998). A later study demonstrated a contribution primarily of longitudinally extensive SC lesions (Amezcua et al., 2013). This lack of evidence contrasts to our finding that SC lesions correlate more closely with EDSS than SC atrophy. Remarkably, a study using a methodology comparable to ours also found an association of SC lesions and EDSS (Weier et al., 2012). Moreover, an independent contribution of whole SC lesion volume and atrophy to disability was observed in a two-center study (Lukas et al., 2013). Regarding our correlation analyses of SC measures with clinical scores, we observed that the time of the 25-Foot Walk Test behaved inversely to the EDSS score in one respect. It was more strongly related to SC atrophy than to SC lesion volume compatible with a very recent study on differences in these clinical scores (Koch et al., 2021). Anatomically plausible, the time of the Nine-Hole Peg Test correlated more strongly with lesion volumes of the upper SC than of the lower SC. Compatible with the fact that arm function declines more slowly than walking (Timmermans et al., 2020), the time of the Nine-Hole Peg Test was not related to SC atrophy in our cohort. As functional (Rocca et al., 2012) and structural (Hagstrom et al., 2017) SC measures had been related to fatigue, we finally tested for such an association but did not observe it.

We acknowledge limitations of our study. Our methods covered the SC from the lower edge of the second vertebra and, hence, not the entire SC. In our cohort, patients in their first year of MS were well represented. The fact that almost 20 percent of patients, assigned for whole SC MRI, were actually not scanned across the whole SC may have introduced a selection bias. We did not analyze diffuse hyperintensities, which however occur later in the disease course making informative results unlikely in our cohort. Our clinical data did not include further SC symptoms such as bladder, bowel, and sexual dysfunction (Ciccarelli et al., 2019).

Our data may be of value to plan further studies. To assess the long-term impact of SC lesions in MS, thorough measurement of SC lesion volume will be necessary. In contrast, SC atrophy may be relatively easy

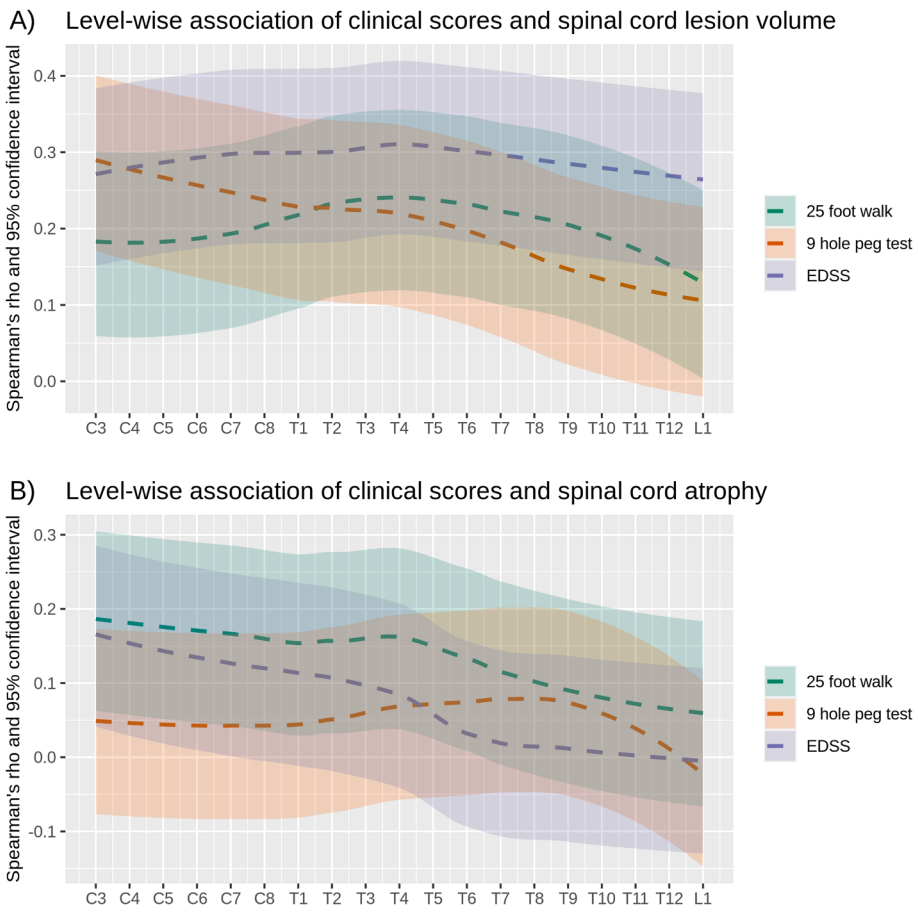

Fig. 6. Association of spinal cord lesions and atrophy with clinical scores across vertebral levels. (A) Level-wise simple non-parametric correlations of Expanded Disability Status Scale (EDSS), 25-Foot Walk Test, and Nine-Hole Peg Test with spinal cord lesion volumes is plotted across vertebral levels (C, cervical; T, thoracic; L, lumbar) for all patients. Of each score, color-coded correlation measures with their 95% confidence intervals (colored areas) are displayed. For visibility, these values were smoothed (default function of ggplot2). Level-wise statistical significance is indicated by non-overlapping confidence intervals with zero. (B) Analogous plots of spinal cord volumes (atrophy) over clinical scores are displayed.

to measure. Studies comparing whole SC volumes with SC sections at several levels may help identify the most efficient and reliable way to estimate SC atrophy – ideally resulting in a commonly accepted standard. Application of structural MRI with higher resolution at large scale may allow to analyze further features of SC lesions such as location within SC cross-sections and involvement of GM and WM (Eden et al., 2019; Schlaeger et al., 2014; Schlaeger et al., 2015). Likewise, more advanced sequences may enable to classify and to better quantify tissue damage (Kearney et al., 2015b; Mariano et al., 2021; Rocca et al., 2020).

We conclude that SC lesions occur in most patients with MS across the whole SC variably but accentuated in the cervical enlargement; they contribute to the clinical picture in the early and late course of MS. In contrast, SC atrophy, spatially, develops more evenly, starting early in the course of MS but contributing to the clinical picture later.

CRediT authorship contribution statement

Matthias Bussas: Formal analysis, Visualization, Writing – review & editing. **Malek El Husseini:** Software, Methodology, Validation. **Laura Harabacz:** Methodology, Data curation, Visualization. **Viktor Pineker:** Methodology, Data curation, Visualization. **Sophia Grahl:** Data curation, Validation, Writing – review & editing. **Viola Pongratz:** Data curation, Validation. **Achim Berthele:** Conceptualization, Writing – review & editing. **Isabelle Riederer:** Data curation, Validation. **Claus Zimmer:** Resources. **Bernhard Hemmer:** Resources. **Jan S. Kirschke:** Conceptualization, Investigation, Methodology, Project administration, Supervision, Writing – review & editing. **Mark Mühlau:** Conceptualization, Investigation, Project administration, Resources, Supervision, Validation, Writing – original draft.

Acknowledgments

This work was supported by the Bavarian State Ministry for Science and Art (Collaborative Bilateral Research Program Bavaria – Québec: AI in medicine, grand F.4-V0134.K5.1/86/34), and in part by the German Research Foundation (DFG SPP2177; Radiomics: Next Generation of Biomedical Imaging; project number 428223038); the National Institutes of Health (grant 1R01NS112161-01); the German Federal Ministry of Education and Research (DIFUTURE: 01ZZ1603[A-D] and 01ZZ1804[A-I]) and the Macroscale Hub of Munich Cluster for Systems Neurology (SyNergy).

References

Amezcua, L., et al., 2013. Spinal cord lesions and disability in Hispanics with multiple sclerosis. J. Neurol. 260, 2770–2776.
Andelova, M., et al., 2019. Additive Effect of Spinal Cord Volume, Diffuse and Focal Cord Pathology on Disability in Multiple Sclerosis. Front. Neurol. 10, 820.
Bonacchi, R., et al., 2020. Clinical Relevance of Multiparametric MRI Assessment of Cervical Cord Damage in Multiple Sclerosis. Radiology 296, 605–615.
Bot, J.C., et al., 2004. Spinal cord abnormalities in recently diagnosed MS patients: added value of spinal MRI examination. Neurology 62, 226–233.
Breckwoldt, M.O., et al., 2017. Increasing the sensitivity of MRI for the detection of multiple sclerosis lesions by long axial coverage of the spinal cord: a prospective study in 119 patients. J. Neurol. 264, 341–349.
Calabrese, P., et al., 2004. Das Multiple Sklerose Inventarium Cognition (MUSIC). Psychoneuro 30, 384–388.
Casserly, C., et al., 2018. Spinal Cord Atrophy in Multiple Sclerosis: A Systematic Review and Meta-Analysis. J. Neuroimaging 28, 556–586.
Ciccarelli, O., et al., 2019. Spinal cord involvement in multiple sclerosis and neuromyelitis optica spectrum disorders. Lancet Neurol. 18, 185–197.
Compston, A., Coles, A., 2008. Multiple sclerosis. Lancet 372, 1502–1517.
Confavreux, C., Vukusic, S., 2006. Natural history of multiple sclerosis: a unifying concept. Brain 129, 606–616.
Eden, D., et al., 2019. Spatial distribution of multiple sclerosis lesions in the cervical spinal cord. Brain 142, 633–646.

Evangelou, N., et al., 2005. Pathological study of spinal cord atrophy in multiple sclerosis suggests limited role of local lesions. Brain 128, 29–34.
Feys, P., et al., 2017. The Nine-Hole Peg Test as a manual dexterity performance measure for multiple sclerosis. Mult. Scler. 1352458517690824.
Filippi, M., et al., 2020. Diagnosis of Progressive Multiple Sclerosis From the Imaging Perspective: A Review. JAMA Neurol.
Galler, S., et al., 2016. Improved Lesion Detection by Using Axial T2-Weighted MRI with Full Spinal Cord Coverage in Multiple Sclerosis. AJNR Am. J. Neuroradiol. 37, 963–969.
Gilmore, C.P., et al., 2006. Spinal cord gray matter demyelination in multiple sclerosis-a novel pattern of residual plaque morphology. Brain Pathol. 16, 202–208.
Hagstrom, I.T., et al., 2017. Relevance of early cervical cord volume loss in the disease evolution of clinically isolated syndrome and early multiple sclerosis: a 2-year follow-up study. J. Neurol. 264, 1402–1412.
Healy, B.C., et al., 2012. Approaches to normalization of spinal cord volume: application to multiple sclerosis. J. Neuroimaging 22, e12–19.
Kearney, H., et al., 2015a. Cervical cord lesion load is associated with disability independently from atrophy in MS. Neurology 84, 367–373.
Kearney, H., et al., 2015b. Spinal cord MRI in multiple sclerosis-diagnostic, prognostic and clinical value. Nat. Rev. Neurol. 11, 327–338.
Kearney, H., et al., 2016. Grey matter involvement by focal cervical spinal cord lesions is associated with progressive multiple sclerosis. Mult. Scler. 22, 910–920.
Keihaninejad, S., et al., 2010. A robust method to estimate the intracranial volume across MRI field strengths (1.5T and 3T). Neuroimage 50, 1427–1437.
Kerbrat, A., et al., 2020. Multiple sclerosis lesions in motor tracts from brain to cervical cord: spatial distribution and correlation with disability. Brain 143, 2089–2105.
Kidd, D., et al., 1993. Spinal cord MRI using multi-array coils and fast spin echo. II. Findings in multiple sclerosis. Neurology 43, 2632–2637.
Klein, J.P., et al., 2011. A 3T MR imaging investigation of the topography of whole spinal cord atrophy in multiple sclerosis. AJNR Am. J. Neuroradiol. 32, 1138–1142.
Koch, M.W., et al., 2021. Comparison of the EDSS, Timed 25-Foot Walk, and the 9-Hole Peg Test as Clinical Trial Outcomes in Relapsing-Remitting Multiple Sclerosis. Neurology.
Lin, X., et al., 2003. The relationship of brain and cervical cord volume to disability in clinical subtypes of multiple sclerosis: a three-dimensional MRI study. Acta Neurol. Scand. 108, 401–406.
Losseff, N.A., et al., 1996. Spinal cord atrophy and disability in multiple sclerosis. A new reproducible and sensitive MRI method with potential to monitor disease progression. Brain 119, 701–708.
Lukas, C., et al., 2013. Relevance of spinal cord abnormalities to clinical disability in multiple sclerosis: MR imaging findings in a large cohort of patients. Radiology 269, 542–552.
Lycklama, G., et al., 2003. Spinal-cord MRI in multiple sclerosis. Lancet Neurol. 2, 555–562.
Mariano, R., et al., 2021. Quantitative spinal cord MRI in MOG-antibody disease, neuromyelitis optica and multiple sclerosis. Brain 144, 198–212.
Mina, Y., et al., 2021. Cervical and thoracic cord atrophy in multiple sclerosis phenotypes: Quantification and correlation with clinical disability. Neuroimage Clin. 30, 102680.
Motl, R.W., et al., 2017. Validity of the timed 25-foot walk as an ambulatory performance outcome measure for multiple sclerosis. Mult. Scler. 1352458517690823.
Nijeholt, G.J., et al., 2001. Post-mortem high-resolution MRI of the spinal cord in multiple sclerosis: a correlative study with conventional MRI, histopathology and clinical phenotype. Brain 124, 154–166.
Nijeholt, G.J., et al., 1998. Brain and spinal cord abnormalities in multiple sclerosis. Correlation between MRI parameters, clinical subtypes and symptoms. Brain 121 (Pt 4), 687–697.
Oh, J., et al., 2014. Spinal cord normalization in multiple sclerosis. J. Neuroimaging 24, 577–584.
Petrova, N., et al., 2018. Axonal loss in the multiple sclerosis spinal cord revisited. Brain Pathol. 28, 334–348.
Poulsen, E.N., et al., 2021. MRI of the Entire Spinal Cord-Worth the While or Waste of Time? A Retrospective Study of 74 Patients with Multiple Sclerosis. Diagnostics (Basel) 11.
Pravatà, E., et al., 2019. Influence of CNS T2-focal lesions on cervical cord atrophy and disability in multiple sclerosis. Mult. Scler. J. 26, 1402–1409.
Qu, Z., et al., 2017. Does the position of conus medullaris change with increased thoracolumbar kyphosis in ankylosing spondylitis patients? Medicine (Baltimore) 96, e5963.
Rocca, M.A., et al., 2012. Abnormal cervical cord function contributes to fatigue in multiple sclerosis. Mult. Scler. 18, 1552–1559.
Rocca, M.A., et al., 2020. What role should spinal cord MRI take in the future of multiple sclerosis surveillance? Expert Rev. Neurother. 20, 783–797.
Schlaeger, R., et al., 2014. Spinal cord gray matter atrophy correlates with multiple sclerosis disability. Ann. Neurol. 76, 568–580.
Schlaeger, R., et al., 2015. Association Between Thoracic Spinal Cord Gray Matter Atrophy and Disability in Multiple Sclerosis. JAMA Neurol 72, 897–904.
Schmidt, P., et al., 2012. An automated tool for detection of FLAIR-hyperintense white-matter lesions in Multiple Sclerosis. Neuroimage 59, 3774–3783.
Sechi, E., et al., 2021. Critical spinal cord lesions associate with secondary progressive motor impairment in long-standing MS: A population-based case-control study. Mult. Scler. 27, 667–673.
Song, X., et al., 2020. Correlation between EDSS scores and cervical spinal cord atrophy at 3T MRI in multiple sclerosis: A systematic review and meta-analysis. Mult. Scler. Relat. Disord. 37, 101426.
Thompson, A.J., et al., 2018. Diagnosis of multiple sclerosis: 2017 revisions of the McDonald criteria. Lancet Neurol. 17, 162–173.
Timmermans, S.T., et al., 2020. Ten-year disease progression in multiple sclerosis: walking declines more rapidly than arm and hand function. Mult. Scler. Related Disord. 45, 102343.
Tsagkas, C., et al., 2018. Spinal cord volume loss: A marker of disease progression in multiple sclerosis. Neurology 91, e349–e358.
Weier, K., et al., 2012. Biplanar MRI for the assessment of the spinal cord in multiple sclerosis. Mult. Scler. 18, 1560–1569.
Yaldizli, O., et al., 2014. The relationship between total and regional corpus callosum atrophy, cognitive impairment and fatigue in multiple sclerosis patients. Mult. Scler. 20, 356–364.